

# Polymetamorphism, zircon growth and retention of early assemblages through the dynamic evolution of a continental arc in Fiordland, New Zealand

J. M. SCOTT, J. M. PALIN, A. F. COOPER, Å. FAGERENG AND R. P. KING

Department of Geology, University of Otago, PO Box 56 Dunedin, New Zealand (jamesscott08@gmail.com)

**ABSTRACT** The Marguerite Amphibolite and associated rocks in northern Fiordland, New Zealand, contain evidence for retention of Carboniferous metamorphic assemblages through Cretaceous collision of an arc, emplacement of large volumes of mafic magma, high-*P* metamorphism and then extensional exhumation. The amphibolite occurs as five dismembered aluminous meta-gabbroic xenoliths up to 2 km wide that are enclosed within meta-leucotonalite of the Lake Hankinson Complex. A first metamorphic event (M1) is manifest in the amphibolite as a pervasively lineated pargasite–anorthite–kyanite or corundum ± rutile assemblage, and as diffusion-zoned garnet in pelitic schist xenoliths within the amphibolite. Thin zones of metasomatically Al-enriched leucotonalite directly at the margins of each amphibolite xenolith indicate element redistribution during M1 and equilibration at  $6.6 \pm 0.8$  kbar and  $618 \pm 25$  °C. A second phase of recrystallization (M2) formed patchy and static margarite ± kyanite–staurolite–chlorite–plagioclase–epidote assemblages in the amphibolite, pseudomorphs of coronas in gabbronorite, and thin high-grossular garnet rims in the pelitic schists. Conditions of M2,  $8.8 \pm 0.6$  kbar and  $643 \pm 27$  °C, are recorded from the rims of garnet in the pelitic schists. Cathodoluminescence imaging and simultaneous acquisition of U–Th–Pb isotopes and trace elements by depth-profiling zircon grains from one pelitic schist reveals four stages of growth, two of which are metamorphic. The first metamorphic stage, dated as  $340.2 \pm 2.2$  Ma, is correlated with M1 on the basis that the unusual zircon trace element compositions indicate growth from a metasomatic fluid derived from the surrounding amphibolite during penetrative deformation. A second phase of zircon overgrowth coupled with crosscutting relationships date M2 to between 119 and 117 Ma. The Early Carboniferous event has not previously been recognized in northern Fiordland, whereas the latter event, which has been identified in Early Cretaceous batholiths, their xenoliths, and rocks directly at batholith margins, is here shown to have also affected the country rock. However, the effects of M2 are fragmentary due to limited element mobility, lack of deformation, distance from a heat source and short residence time in the lower crust during peak *P* and *T*. It is possible that many parts of the Fiordland continental arc achieved high-*P* conditions in the Early Cretaceous but retain earlier metamorphic or igneous assemblages.

**Key words:** Fiordland; metamorphism; metastability; zircon REE; zircon U–Pb.

## INTRODUCTION

The complex interplay of polyphase metamorphism, magmatism and deformation along convergent margins makes resolving the geological history difficult because recrystallization results in obliteration or retrogression of early mineral assemblages. Problems in reconstructing the nature and extent of polyphase metamorphic events are exemplified in the long-lived convergent history of the paleo-Pacific Gondwana continental margin preserved in New Zealand. The Fiordland segment of this margin (Fig. 1) contains a complex Phanerozoic evolution culminating in Early Cretaceous collision of a magmatic arc and emplacement of the > 3000 km<sup>2</sup> Arthur River Complex (ARC) (136–129 Ma) and Western Fiordland Orthogneiss (WFO) (126–116 Ma) mafic batholiths, accompanied by

high-*P* granulite facies metamorphism (123–113 Ma), and then extensional exhumation (111–90 Ma) (Mattinson *et al.*, 1986; Gibson *et al.*, 1988; Bradshaw, 1989, 1991; Gibson & Ireland, 1995; Clarke *et al.*, 2000; Daczko *et al.*, 2001a,b, 2002b; Flowers *et al.*, 2005; Scott & Cooper, 2006). Despite widespread and voluminous emplacement of mafic magma into the middle and lower crust, much of the Fiordland country rock contains metamorphic mineral assemblages of low, moderate or unquantified pressure characteristics (Oliver, 1977; Gibson, 1990; Bradshaw, 1989, 1991; Brown, 1996; Ireland & Gibson, 1998; Davids, 1999).

To investigate the evolution of the northern Fiordland continental arc, this study examines the metamorphic properties of an aluminous meta-gabbro (Marguerite Amphibolite), pelitic schist xenoliths,

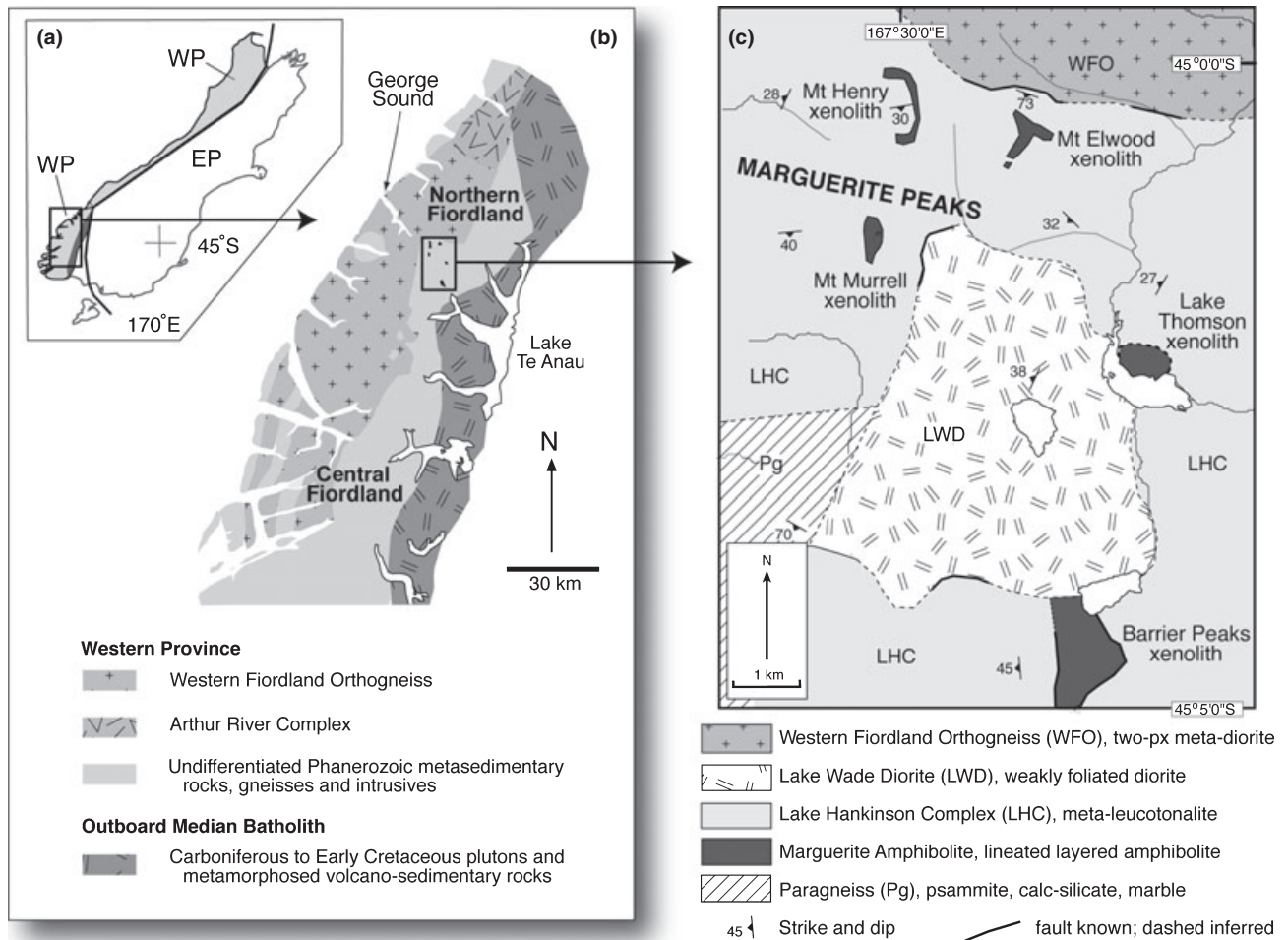


**Fig. 1.** (a) Simplified subdivision of basement geology in the Eastern Province (EP) and Western Province (WP) in the South Island of New Zealand. (b) Simplified geological map of Fiordland. Data from Allibone *et al.* (2007). (c) Geological map of the Marguerite Amphibolite. Data from King (1984).

and meta-leucotonalite host rocks (Lake Hankinson Complex), exposed 1–9 km from the WFO (Fig. 1). Minerals in aluminous meta-gabbros and schists are sensitive to subtle changes in pressure, temperature and fluid conditions (e.g. Chatterjee *et al.*, 1984; Spear *et al.*, 1999; Arnold *et al.*, 2000; Clarke *et al.*, 2000; Daczko *et al.*, 2002a,c; Tsujimori & Liou, 2004) and thus allow the possibility of determining the  $P$ – $T$  evolution in a region dominated by low variance assemblages. Integration of the  $P$ – $T$  data with zircon U–Th–Pb isotope and trace element concentrations obtained by depth-profiling zoned grains by LA–ICP–MS (laser ablation inductively coupled plasma mass spectrometry) show that Carboniferous assemblages persevered through Cretaceous magmatism and tectonism despite the latter event reaching upper amphibolite to granulite facies conditions. These results suggest that where there is evidence for a lack of deformation, fluid and short duration of peak conditions, observed metamorphic assemblages might not record the  $P$ – $T$  evolution.

## GEOLOGICAL FRAMEWORK

New Zealand basement geology comprises an amalgamation of terranes accreted to the Gondwana supercontinent in the Phanerozoic. These terranes are subdivided into the Eastern Province and Western Province (Landis & Coombs, 1967; Mortimer, 2004) separated by the Outboard Median Batholith magmatic arc (Bradshaw, 1993; Kimbrough *et al.*, 1994; Mortimer *et al.*, 1999a, 1999b) (Fig. 1). The Eastern Province is composed of Mesozoic terranes merged in a Cretaceous accretionary prism (Mortimer, 2004; Wandres & Bradshaw, 2005). The Western Province consists of the Early Palaeozoic Buller and Takaka terranes from which detrital zircon age spectra indicate formation on the Gondwana peri-cratonic margin (Gibson & Ireland, 1996; Ireland & Gibson, 1998; Jongens *et al.*, 2003; Hollis *et al.*, 2004). The terrane subdivision is not yet clear in northern Fiordland because this area exposes a deeper crustal section, but detrital zircon studies show that most Fiordland

metasedimentary rocks belong to the Western Province (Gibson & Ireland, 1996; Ireland & Gibson, 1998).

Parts of the Fiordland Western Province were affected by metamorphism attaining moderate pressures (3–7 kbar) in the Devonian and/or Carboniferous (Gibson & Ireland, 1996; Ireland & Gibson, 1998; Davids, 1999; Daczko *et al.*, 2009). This event was associated with formation of a penetrative fabric and isoclinal folding (Gibson, 1982) and pre-, syn- and post-tectonic emplacement of plutonic rocks (Davids, 1999; Allibone *et al.*, 2007). Tectonic quiescence ensued until intrusions of Early Cretaceous portions of the gabbroic-monzodioritic ARC and then the extensive (>3000 km<sup>2</sup>) WFO (Mattinson *et al.*, 1986; Bradshaw, 1989, 1990; Hollis *et al.*, 2003, 2004). These two units together comprise approximately half of the exposed geology. The trigger behind emplacement of the ARC and WFO may be the juxtaposition of an outboard magmatic arc with the Gondwana margin (Muir *et al.*, 1998; Daczko *et al.*, 2001a; Scott, 2008). This arc, known as the Outboard Median Batholith, is represented by a belt of subduction-related Carboniferous to Cretaceous plutons and meta-volcanosedimentary rocks on the eastern side of Fiordland (Williams, 1978; Williams & Harper, 1978; Blattner, 1991; Muir *et al.*, 1998; Blattner & Graham, 2000; Ewing *et al.*, 2007; Scott & Palin, 2008; Scott *et al.*, 2008).

Following and during WFO emplacement, parts of Fiordland experienced garnet granulite facies metamorphism (Oliver, 1977; Mattinson *et al.*, 1986; Bradshaw, 1989, 1990; Gibson & Ireland, 1995; Brown, 1996; Daczko *et al.*, 2001a,b, 2002a,b; Hollis *et al.*, 2004). High-*P* conditions are recorded by scattered dehydration zones of garnet and clinopyroxene formed from hornblende and clinozoisite breakdown in meta-dioritic lithologies (Oliver, 1977; Clarke *et al.*, 2000; Daczko *et al.*, 2001b, 2002b; Daczko & Halpin, 2009). These textures occur in <10% of the WFO-ARC, with the remainder composed of unmetamorphosed igneous rock, auto-metamorphic garnet-absent granulite or retrogressed amphibolite (Bradshaw, 1989, 1990; Brown, 1996). Geothermobarometry coupled with U-Pb geochronology indicates that the garnet granulite facies event represents mid-Cretaceous loading of the crust by between 2 and 6 kbar overburden (Mattinson *et al.*, 1986; Bradshaw, 1989; Brown, 1996; Clarke *et al.*, 2000; Daczko & Halpin, 2009). Other evidence for a high-*P* event comes from pelitic schists on the margins of, and as xenoliths within, the WFO. These rocks often have high-grossular garnet rims ( $\geq 9$  kbar) as overgrowths around diffusion-zoned cores (Bradshaw, 1989, 1991; Brown, 1996). However, this type of garnet zoning is also recognized well away from the WFO in country rock interpreted to have been metamorphosed in the middle Palaeozoic (Davids, 1999). Isobaric cooling between 113 and 111 Ma is recorded by kyanite–plagioclase–quartz pseudomorphs of high-*P* assemblages in northern Fiordland (Daczko

*et al.*, 2002c; Flowers *et al.*, 2005). The convergent orogen had collapsed by 111–108 Ma and extensional detachment faults rapidly exhumed the lower crust back to middle and upper crustal depths (Gibson *et al.*, 1988; Scott & Cooper, 2006; Klepeis *et al.*, 2007). Final exhumation took place in the Neogene (Claypool *et al.*, 2002; House *et al.*, 2002, 2005).

## FIELD RELATIONSHIPS

Marguerite Amphibolite crops out as five xenoliths of variably metamorphosed aluminous gabbro which are totally enclosed within the meta-leucotonalite Lake Hankinson Complex in the Marguerite Peaks in northern Fiordland (Fig. 1c) (King, 1984). Each xenolith is <2 km wide or long. Thin zones of hybrid aluminous Lake Hankinson Complex leucotonalite occur at some contacts. The dominant lithology in each xenolith is layered amphibolite composed of centimetre- to decimetre-scale horizons of cream-white plagioclase or epidote, alternating with green amphibole (Fig. 2a). Red corundum porphyroblasts are scattered throughout (Fig. 2b), and mineral lineations are pervasive (Fig. 2c). Several patches of pale grey–green gabbro occur in scattered low strain domains in the southwestern portion of the Mt Murrell xenolith. These zones are up to 3 m wide and grade into amphibolite (Fig. 2d). Small patches of garnetiferous pelitic, semi-pelitic, amphibolitic and calc-silicate gneiss occur as xenoliths within the layered amphibolite and represent the country rock to which the amphibolite was intruded. Massive hornblende gabbro sills cut the Mt Murrell xenolith and granitic pegmatite dykes intrude all xenoliths (Scott *et al.*, in press).

## MINERALOGY

Representative key lithologies were analysed by energy dispersive spectrometry on a JEOL JXA-8600 Superprobe housed in the University of Otago (OU) Geology Department and by wavelength dispersive spectrometry on a JEOL JXA-8900R Superprobe housed at the University of Nevada Las Vegas (UNLV) Department of Geosciences. The OU microprobe has two spectrometers and was operated using a beam diameter of 5–20  $\mu\text{m}$  at 1 nA current and 15 kV accelerating voltage. The UNLV microprobe has three spectrometers and was operated using a beam of 5  $\mu\text{m}$  diameter at 20 nA current and 30 kV accelerating voltage. Data were reduced using ZAF corrections. Mineral abbreviations follow Siivola & Schmidt (2007). Amphibole classification follows Leake *et al.*, (1997).

### Lake Hankinson Complex meta-leucotonalite

Al-enriched Lake Hankinson Complex meta-leucotonalite (Fig. 3a) at the margin of the Mt Murrell xenolith

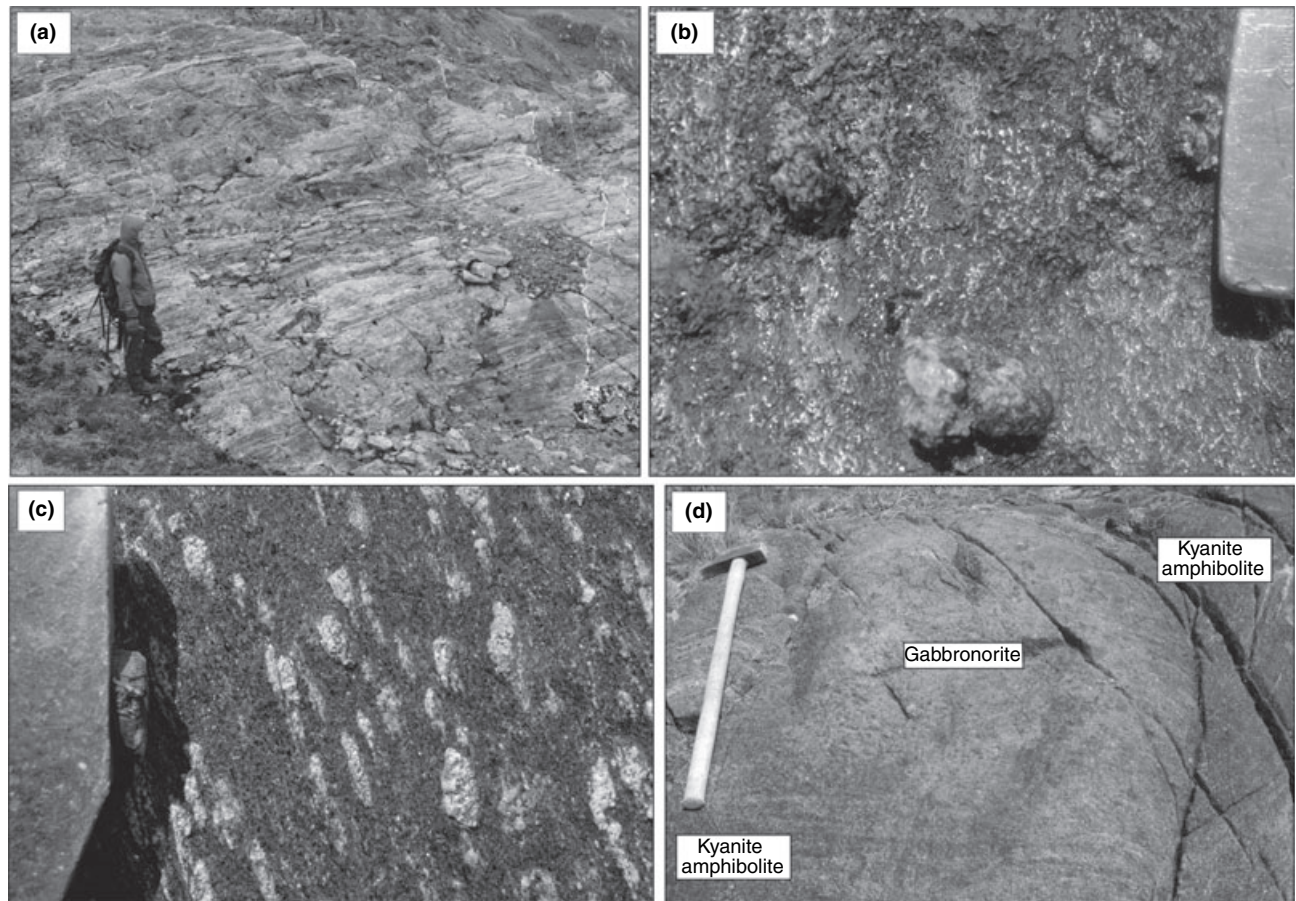


**Fig. 2.** (a) Layered amphibolite in the Mt Elwood xenolith. (b) Corundum porphyroblasts in amphibolite. Exposed section of hammer at top right is 4 cm long. (c) Lineated amphibolite. White spots are aggregates of kyanite and margarite replacing lineated corundum and/or anorthite. (d) Low strain gabbronorite pod surrounded by, and grading into, kyanite amphibolite. Hammer is 1 m long.

contains poikiloblastic Fe–Mg-rich garnet grains lacking systematic zonation [ $\text{alm}_{59-64}\text{prp}_{24-31}\text{grs}_{8-10}\text{sps}_{1-2}$  where  $\text{alm}$  = almandine =  $100\text{Fe}/(\text{Mg} + \text{Fe} + \text{Ca} + \text{Mn})$ ;  $\text{prp}$  = pyrope =  $100\text{Mg}/(\text{Mg} + \text{Fe} + \text{Ca} + \text{Mn})$ ;  $\text{grs}$  = grossular =  $100\text{Ca}/(\text{Mg} + \text{Fe} + \text{Ca} + \text{Mn})$ ;  $\text{sps}$  = spessartine =  $100\text{Mn}/(\text{Mg} + \text{Fe} + \text{Ca} + \text{Mn})$ ] set amongst ferro-pargasite ( $X_{\text{Mg}} = 100\text{Mg}/(\text{Mg} + \text{Fe}) = 43-48$ ), biotite ( $X_{\text{Mg}} = 69-72$ ), andesine ( $\text{ab}_{60-65}\text{an}_{35-40}\text{or}_0$ ) [where  $\text{an}$  = anorthite =  $100\text{Ca}/(\text{Ca} + \text{Na} + \text{K})$ ;  $\text{ab}$  = albite =  $100\text{Na}/(\text{Ca} + \text{Na} + \text{K})$ ;  $\text{or}$  = orthoclase =  $100\text{K}/(\text{Ca} + \text{Na} + \text{K})$ ], gedrite, kyanite and quartz. Zircon, apatite and ilmenite are accessory phases.

#### Layered Marguerite Amphibolite

The principal layered amphibolite lithology consists of pleochroic pargasite ( $Z$  = grass green,  $X$  = very pale green) ( $X_{\text{Mg}} = 55-59$ ;  $\text{Si pfu} = 6.35-6.24$ ), anorthite ( $\text{an}_{92-93}\text{ab}_{8-7}\text{or}_0$ ) and either kyanite or corundum (Fig. 3b). Kyanite and corundum were not observed in textural equilibrium with one

another, although both occur separately in sharp contact with pargasite and anorthite. Rutile is an accessory phase. This pervasive lineated assemblage has partially statically recrystallized to margarite, chlorite, epidote, staurolite and second generation kyanite and plagioclase (Fig. 3c,d). Margarite ( $\text{mrg}_{85-91}\text{pg}_{9-15}\text{ms}_{0-1}$ ) [where  $\text{mrg}$  = margarite =  $100\text{Ca}/(\text{Ca} + \text{Na} + \text{K})$ ;  $\text{pg}$  = paragonite =  $100\text{Na}/(\text{Ca} + \text{Na} + \text{K})$ ;  $\text{ms}$  = muscovite =  $100\text{K}/(\text{Ca} + \text{Na} + \text{K})$ ] occurs as randomly oriented sheaves commonly associated with kyanite and epidote. Corundum porphyroblasts are partially replaced by kyanite, margarite and strongly pleochroic yellow staurolite. Second generation kyanite is finer grained and more prismatic than the first generation but chemically indistinguishable. Early anorthite is either pseudomorphed by epidote or has thin rims of oligoclase-andesine composition ( $\text{an}_{23-45}$ ; King, 1984). Pale green to colourless Mg-chlorite ( $X_{\text{Mg}} = 86$ ) partially replaces pargasite. Quartz occurs rarely and only in association with margarite.

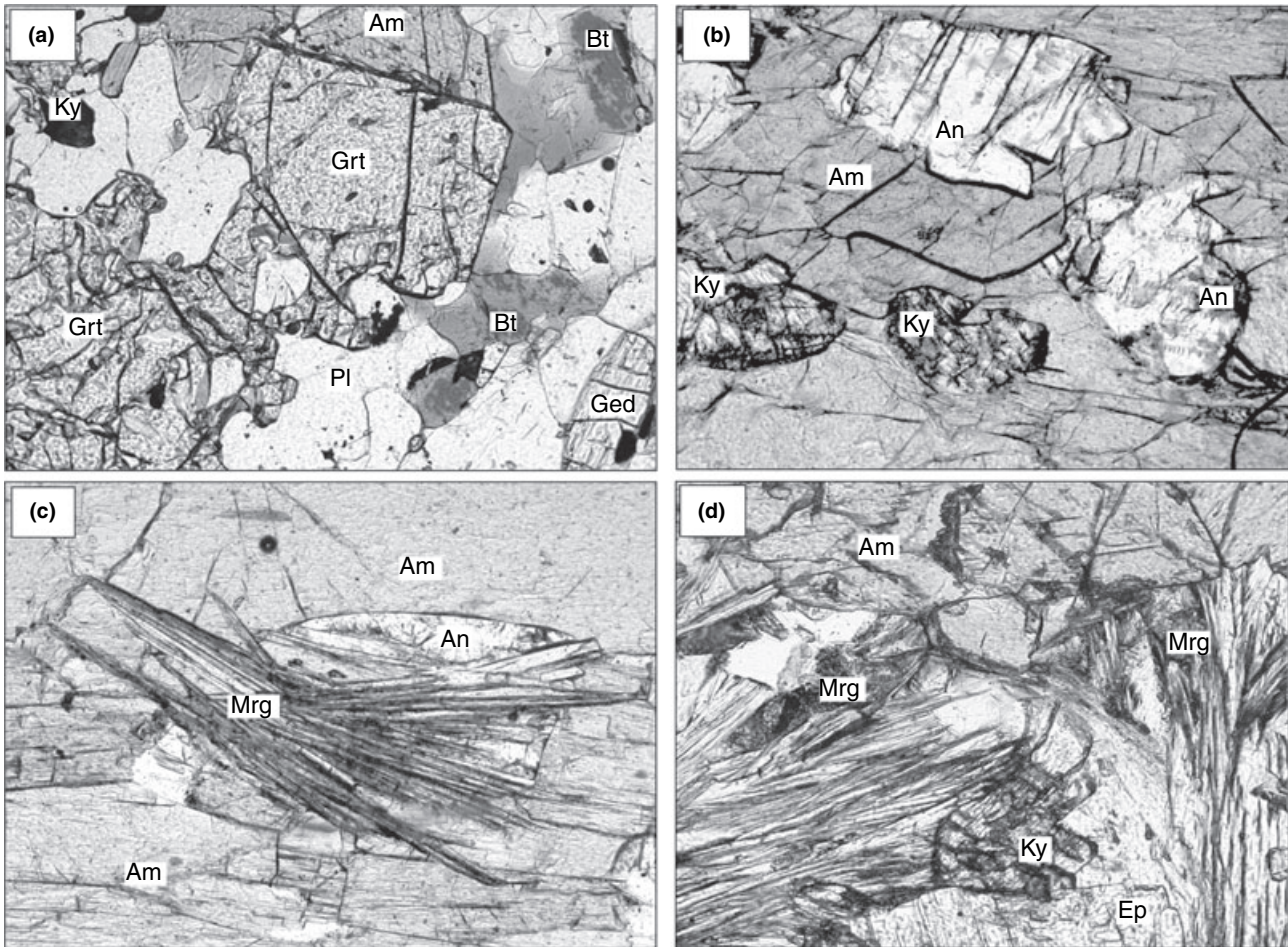


**Fig. 3.** (a) Lake Hankinson Complex meta-leucotonalite M1 assemblage. Width of view is 1 mm. (b) Layered M1 assemblage in layered amphibolite. Width of view is 2 mm. (c) Sheafs of M2 Mrg overgrowing M1 Am and An. Width of view is 0.5 mm. (d) Randomly oriented M2 Mrg and Ky after M1 Am and An. Width of view is 0.7 mm.

### Marguerite Amphibolite gabbronorite

Gabbronorite from the core of one of the low strain zones dispersed amongst the layered amphibolite (Fig. 2d) contains amphibole–spinel symplectic coronas at anorthite–olivine interfaces (Fig. 4a). In fresh samples, these coronas consist of a core of olivine ( $X_{Mg} = 77–78$ ) surrounded by orthopyroxene ( $X_{Mg} = 72–80$ ;  $SiO_2 = 54.02–56.24$  wt%), enclosed within a symplectic shell of pale green pargasite and/or edenite ( $X_{Mg} = 56–67$ ;  $SiO_2 = 43.55–43.86$  wt%) and pleonaste spinel ( $X_{Mg} = 52–54$ ). Pale green-brown amphibole grains enclose anorthite ( $an_{93–98}ab_{2–7}or_0$ ), clinopyroxene ( $X_{Mg} = 74–80$ ;  $Cr_2O_3 = 0.28–0.67$  wt%) and the amphibole–spinel symplectites. Rare earth element and isotopic analyses of similar coronas have been interpreted to show formation during late-stage magmatic processes (de Haas *et al.*, 2002). With progression away from the centre of the gabbronorite low strain domains, metamorphic minerals pseudomorph primary minerals (Fig. 4b). Seriate pale green amphibole completely replaces olivine–

orthopyroxene corona cores through to sites formally occupied by amphibole–spinel symplectite. Amphibole near the cores has  $X_{Mg} = 62–74$  and  $SiO_2 = 51.88$  wt%, similar to the composition of the original orthopyroxene. Primary anorthite has been totally replaced by sheaf-like aggregates of randomly oriented margarite ( $mrg_{85–89}pg_{11–15}ms_{0–1}$ ) and prisms of euhedral kyanite and epidote with or without pale green chlorite (Fig. 4b,c). Amphibole that replaces the symplectites has  $X_{Mg} = 52–55$  and  $SiO_2 = 44.10$  wt%, similar to amphibole from the original symplectite. Igneous Cr–clinopyroxene is replaced by pale green Cr–amphibole ( $Cr_2O_3 = 0.22–0.51$  wt%) (Fig. 4d).

### Pelitic schist xenoliths

Pelitic schist xenoliths up to several metres diameter in the Barrier Peaks body contain 1 to 3 mm diameter garnet porphyroblasts set in a matrix of biotite, kyanite, staurolite, plagioclase and quartz. Garnet CaO concentrations decrease away from the core (e.g.

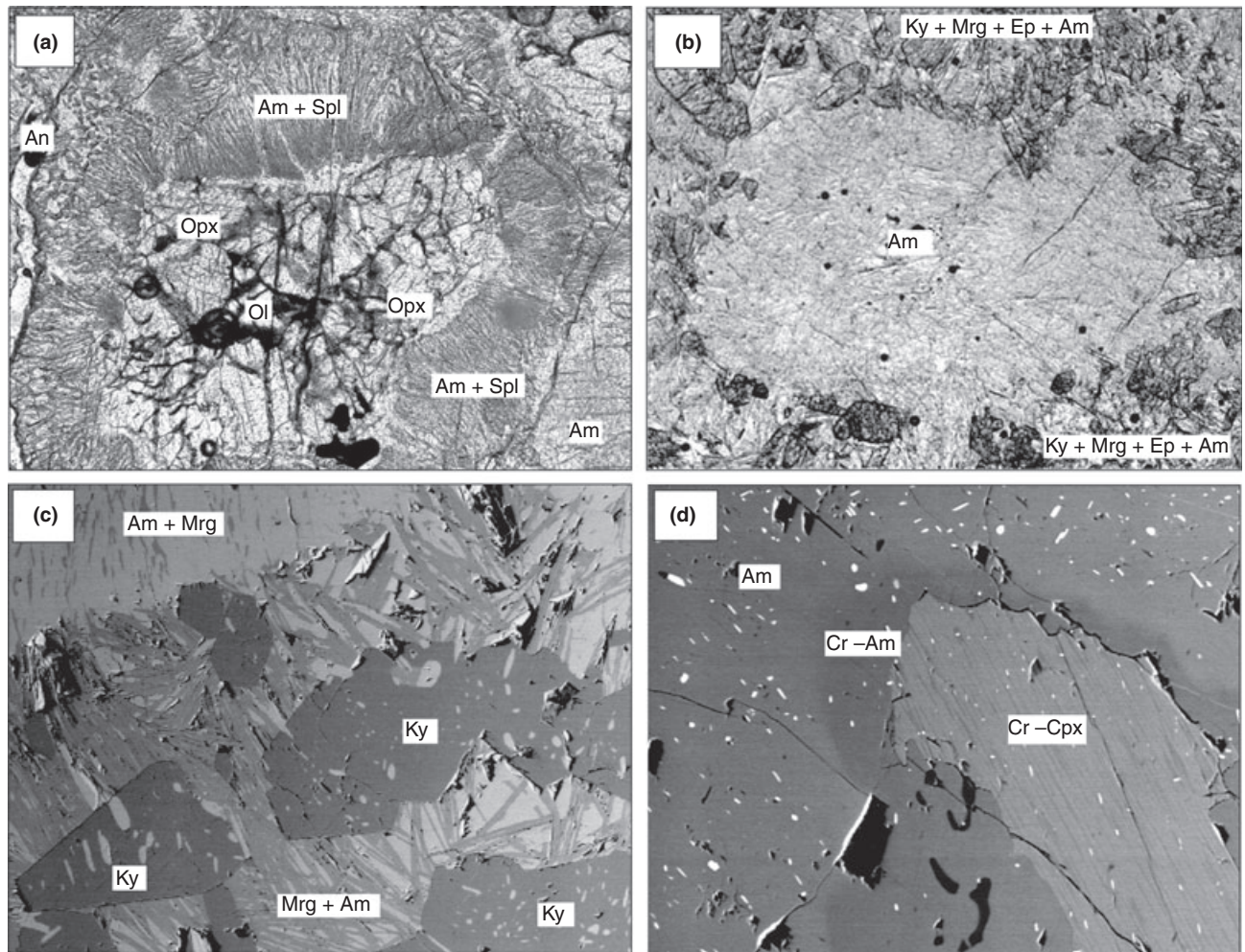


**Fig. 4.** (a) Relict gabbronorite with opx–Am–Spl coronas formed at Ol–An interfaces. Width of view is 3 mm. (b) Gabbronorite corona pseudomorphed by M2 assemblage. Width of view is 2 mm. (c) Backscatter electron image of Ky and Mrg after An in a meta-gabbronorite. In the upper left corner, the original Am–Spl portion of the corona has been pseudomorphed by M2 Am and Mrg. Width of view is 0.25 mm. (d) Partial replacement of igneous Am and Cr–Cpx by metamorphic Am.

alm<sub>72</sub>prp<sub>18</sub>grs<sub>7</sub>sps<sub>3</sub> to alm<sub>75</sub>prp<sub>18</sub>grs<sub>5</sub>sps<sub>2</sub>) but abruptly increase at the rims (e.g. alm<sub>73</sub>prp<sub>16</sub>grs<sub>10</sub>sps<sub>1</sub>). CaO X-ray element maps show the high-grossular rims to be thin and patchily developed but to truncate diffusion-zoned (Tracy, 1982) cores (Fig. 5). The high-grossular garnet rims are in contact with biotite ( $X_{Mg} = 47–55$ ), oligoclase (ab<sub>73–79</sub>an<sub>20–26</sub>or<sub>0–1</sub>), kyanite and staurolite. Rutile, ilmenite and zircon are accessory phases. High-grossular garnet rims in other pelitic schists in Fiordland have been interpreted as indicating attainment of high-*P* conditions (Bradshaw, 1989, 1991; Brown, 1996; Davids, 1999).

#### METAMORPHIC HISTORY & THERMOBAROMETRY

Petrographic data outlined above indicate that two discrete metamorphic events affected the Marguerite Amphibolite and related rocks. These episodes are

termed M1, which is associated with formation of lineated assemblages, and M2, which represents patchy re-equilibration under static conditions (Table 1). The pelitic schist xenolith is interpreted to record this two-stage evolution with the diffusion-zoned cores to garnet representing M1 and the thin high-grossular rims and statically grown matrix representing M2. Because the hybrid Lake Hankinson Complex meta-leucotonalite on the margins of the Marguerite Amphibolite xenoliths is lineated and lacks garnet with high-grossular rims, zoned minerals or static recrystallization textures, *P–T* estimates obtained from these rocks most likely formed during M1. Garnet–biotite 5AV (GB) and garnet–aluminosilicate–silica–plagioclase (GASP) geothermobarometry (Holdaway, 2000, 2001) conducted on six sets of garnet rims paired to adjacent plagioclase, biotite and quartz in sample OU 41466 yielded averaged estimates of  $6.6 \pm 0.8$  kbar and  $618 \pm 25$  °C (representative analyses in Table 2).

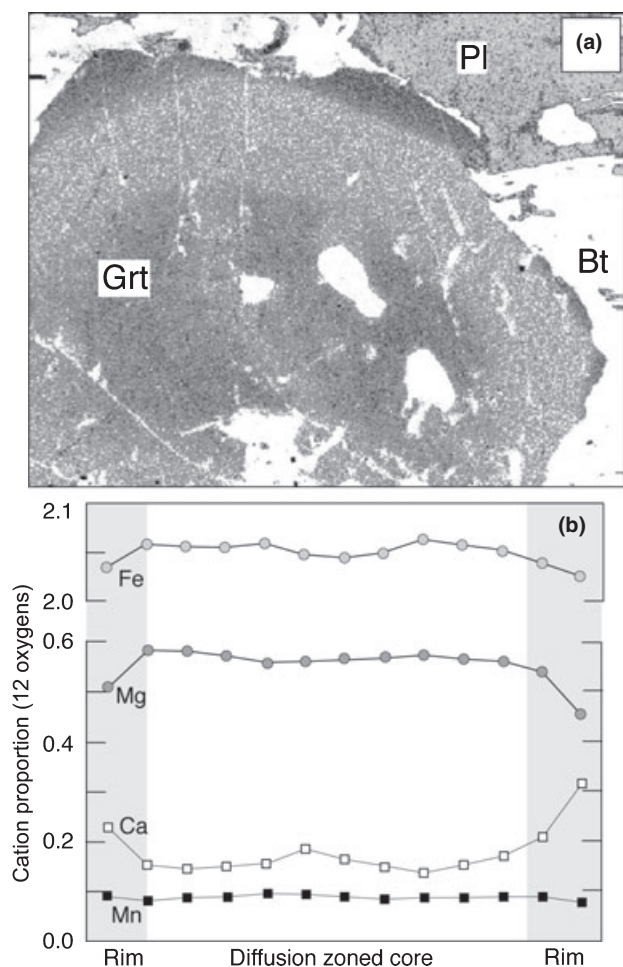


**Fig. 5.** (a) X-ray CaO element map of a zoned garnet from pelitic schist xenolith sample OU 41573. Darker colour corresponds to increase in CaO concentration. Width of view is 0.5 mm. (b) Compositional variation across a zoned garnet grain from same sample. Concentrations were determined quantitatively.

**Table 1.** Summary of metamorphic assemblages and metamorphic events.

Lithology	Metamorphic assemblage	
	M1 lineated	M2 static
Layered amphibolite	An-Prg-Ky or Co-Rt	Mrg-Ep-St-Pl-Ky-Chl
Gabbronorite	Not observed	Mrg-Ep-Ky-Prg-Chl
Pelitic schist xenolith	Low-grs Grt interiors	High-grs Grt rims-Bt-Ky-Pl-Qtz
Meta-leucotonalite	Grt-Ky-Bt-Pl-Qtz-Prg-Ged	Not observed
<i>P-T</i> estimates	6.6 ± 0.8 kbar, 618 ± 25 °C	8.8 ± 0.6, 643 ± 27 °C

Restriction of the aluminous meta-leucotonalite to a thin zone where it contacts the Marguerite Amphibolite suggests that the leucotonalite was enriched in  $Al_2O_3$  from the contiguous amphibolite, and that M1 was accompanied by a redistribution of elements.

The M2 assemblages developed under static conditions and the preservation of igneous mineral ratios in

**Table 2.** Representative mineral analyses used in geothermobarometry.

Sample	Meta-leucotonalite			Pelitic schist		
	99 2 3 Grt rim	5 2 3 Bt matrix	22 2 c3 Pl matrix	150 4 1 Grt rim	28 4 1 Bt matrix	44 4 1 Pl matrix
SiO <sub>2</sub>	37.71	38.24	58.01	37.77	36.16	63.47
Al <sub>2</sub> O <sub>3</sub>	22.94	19.58	26.00	20.50	19.57	22.95
TiO <sub>2</sub>	bdl	1.33	bdl	0.01	1.72	0.02
FeO	28.81	11.92	bdl	33.22	18.02	0.06
MnO	1.03	0.00	bdl	0.67	0.03	bdl
MgO	6.64	15.29	bdl	4.24	11.57	bdl
CaO	2.99	bdl	8.35	3.11	0.05	4.28
Na <sub>2</sub> O	0.01	0.39	6.98	0.01	0.33	9.52
K <sub>2</sub> O	bdl	8.89	0.04	bdl	7.82	0.09
Total	100.13	95.63	99.38	99.53	95.25	100.39
O basis	12	12	8	12	12	8
Si	2.94	3.12	2.61	3.02	3.05	2.80
Al	2.11	0.13	1.38	1.94	0.17	1.19
Ti	0.00	1.20	0.00	0.00	1.24	0.00
Fe	1.88	0.81	0.00	2.22	1.27	0.00
Mn	0.07	0.00	0.00	0.05	0.00	0.00
Mg	0.77	1.86	0.00	0.51	1.45	0.00
Ca	0.25	0.00	0.40	0.27	0.00	0.20
Na	0.00	0.06	0.61	0.00	0.05	0.81
K	0.00	0.93	0.00	0.00	0.84	0.01
Total	8.01	8.11	5.01	8.01	8.08	5.01

bdl, below detection limit.

the pseudomorphed gabbronorite coronas indicate element mobility was restricted. Thin and discontinuous high-grossular garnet rims and the static matrix in the pelitic schist (Fig. 5) represent M2 growth. GB-GASP geothermobarometry for 11 sets of high-grossular rim paired with adjacent plagioclase, biotite and quartz, and guided by CaO X-ray maps, yielded results of  $9.0 \pm 0.8$  kbar and  $643 \pm 37$  °C. Average *P-T* conditions were also calculated using THERMOCALC version 3.3 following the method of Powell & Holland (1994) and the internally consistent thermodynamic dataset of Holland & Powell (1998) (version ds55). End member activities were calculated with AX version 0.3. The albite end member was automatically eliminated by THERMOCALC, and Mg-staurolite end member was eliminated manually because of its low activity. Five independent reactions gave *P-T* conditions of  $8.6 \pm 1.0$  kbar and  $644 \pm 38$  °C with fit values indicating the result is within calculated uncertainty at the 95% confidence level. M2 in the Marguerite Amphibolite and associated rocks is therefore interpreted to have occurred at  $8.8 \pm 0.6$  kbar,  $643 \pm 27$  °C, which is the weighted average of both geothermobarometric results at the 95% confidence level.

## TIMING OF METAMORPHISM

It is important to know the age of the two phases of metamorphism in order to understand their tectonic context. Complexly zoned zircon grains were extracted from a small pelitic schist xenolith hosted within M1- and M2-affected amphibolite. Grains were imaged under cathodoluminescence (Fig. 6) at the University of Otago Geology Department and then dated by LA-ICP-MS at the Australian National

University following the method outlined in Scott & Palin (2008). The metamorphic rims, which are too thin to be analysed by the standard procedure of ablating a polished grain in cross-section, were measured by mounting the zircon in epoxy and grinding the mount until about only one third of each grain remained. The extra abrasion allowed the laser beam to ablate from the zircon interior through to the rim (Fig. 7). All data were standardized against TEMOR-A-2 and NIST 610. U–Th–Pb data are presented in Table S1. Due to the difference between measured and expected  $^{208}\text{Pb}/^{238}\text{U}$  against measured  $^{232}\text{Th}/^{238}\text{U}$ , most grains were estimated to contain a small amount of common Pb (Compston *et al.*, 1984) and so all discussed dates and pooled ages have had a  $^{208}\text{Pb}$  correction applied. A concordia diagram for the  $^{208}\text{Pb}$  corrected dataset is shown in Fig. 8. All quoted ages are reported at  $2\sigma$ . During acquisition of U–Th–Pb isotopes, the concentrations of Th, La, Ce, Sm, Eu, Dy, Lu, P, Hf, Zr and Y were simultaneously collected. This method allows element concentrations to be precisely attributed to growth zones and has the advantage that both age and element data were collected and standardized under the exact same operating conditions. A disadvantage is that only a subset of rare earth

elements (REE) was collected, although remaining values can be interpolated following the method of Ballard *et al.* (2002).

### Stage 1 zircon

The oldest five dates, between 999 and 444 Ma (Table S1), are from the cores of oscillatory-zoned grains (Fig. 6a). Three of these five dates have high internal mean squared weighted deviates (MSWD), indicating the internal U–Pb isotope systematics may have been partially affected and the reported age may be neither accurate nor precise. This may be a result of the  $\leq 10\ \mu\text{m}$  thick overgrowths that truncate all zoned cores.

### Stage 2 zircon

Fifteen dull luminescent grains with faint oscillatory zonation have a pooled age of  $350.6 \pm 2.6\ \text{Ma}$  (MSWD = 1.4). The presence of oscillatory zonation abruptly truncated by a metamorphic overgrowth (Fig. 6b,c,e–h) suggests that these grains were initially larger and were either abraded in the sedimentary cycle prior to development of the metamorphic rim or partially resorbed. Analyses within this population have

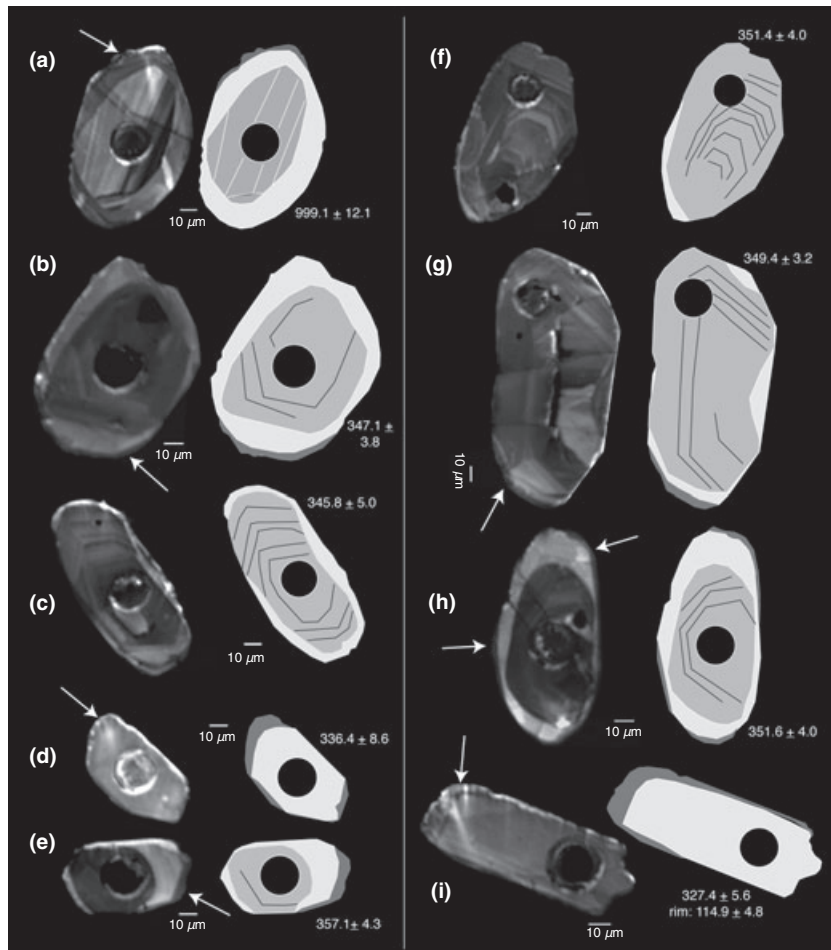


**Fig. 6.** (a–i) Cathodoluminescence images and sketches of zoned zircon grains from OU 41573. Different shades of grey represent different stages of growth. The pits in each grain indicate the site of U–Th–Pb and REE analysis. Arrows indicate Stage 4 rims. Bright patches on some rims are caused by the cathodoluminescence light source.

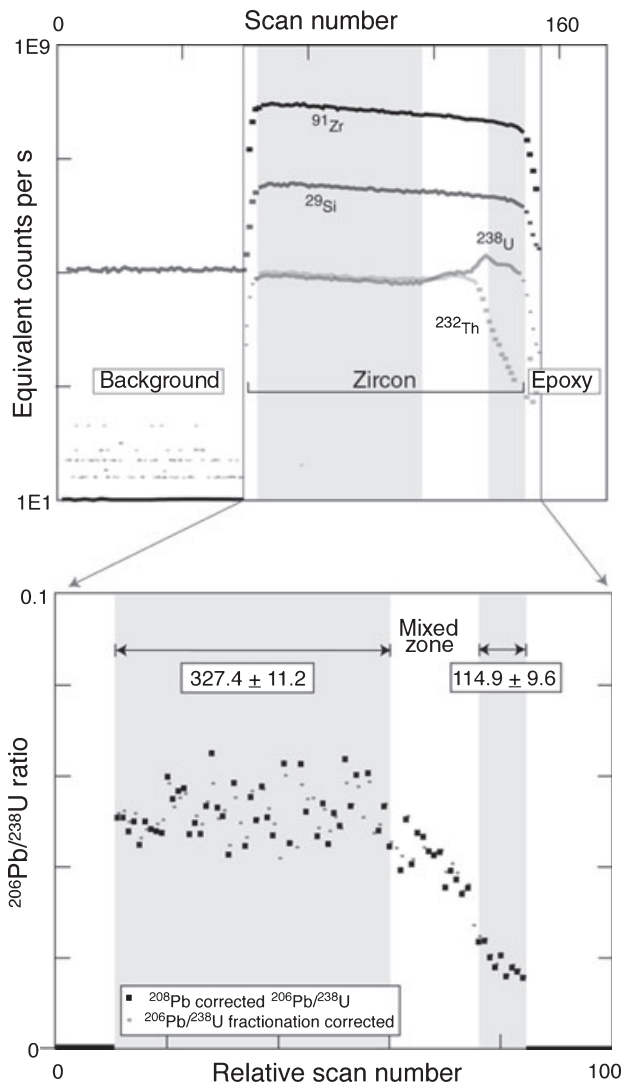


Fig. 7. Example of a depth-profile from core to rim of one zircon grain from the pelitic schist (analysis no. 28; Table S1).

positive interpolated Ce/Ce\* and negative interpolated Eu/Eu\* anomalies (Fig. 9a).

### Stage 3 zircon

Thirty-seven brightly luminescent areas lacking any form of zoning occur as overgrowths to Stages 1 and 2 (Fig. 6a–c,e,g,h) and as single grains (Fig. 6d,i). This population has a pooled U–Pb age of  $340.2 \pm 2.2$  Ma (MSWD = 1.4). Relative to the Stage 2 zircon, Stage 3 analyses have distinctly lower Eu and Ce concentrations (Fig. 9b) and higher average Th/U (1.6 compared to 0.8). This Th/U ratio is also higher than typical for metamorphic zircon (< 0.1; e.g. Schaltegger *et al.*, 1999; Hoskin & Black, 2000; Rubatto *et al.*, 2001; Hoskin & Schaltegger, 2003), although a low ratio is not always diagnostic (e.g. Möller *et al.*, 2003; Kelly & Harley, 2005; Harley *et al.*, 2007). Stage 3

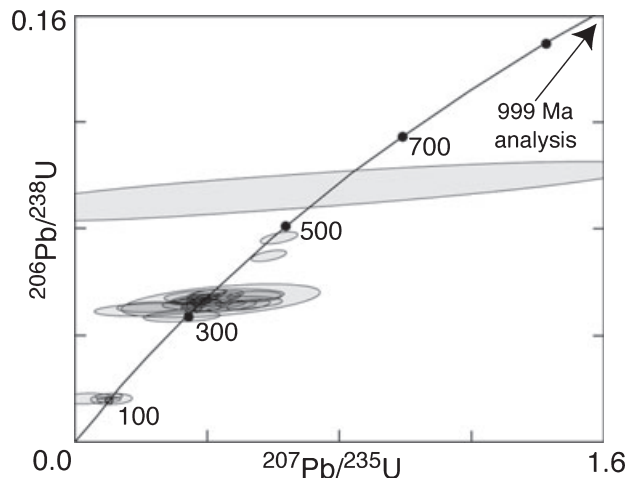


Fig. 8. Concordia diagram for zircon analyses from sample OU 41573. Discordant data omitted.  $^{208}\text{Pb}$  correction applied. Ellipses represent  $1\sigma$  on individual dates.

zircon analyses have total mol Y + heavy REE concentrations similar to Stage 2, but higher P concentrations (Fig. 9d).

### Stage 4 zircon

Very thin and patchily developed darkly luminescent zones occur on the rims of Stages 1, 2 and 3 (Fig. 6a,b,d,e,g–i). Just prior to the laser ablating through the grain into epoxy, the U–Pb isotope ratios changed from Carboniferous to Cretaceous with a mixed intermediate zone (e.g. Fig. 7). The intermediate zones probably represent sites of incomplete homogenization during metamorphism rather than meaningful periods of growth (e.g. Hoskin & Black, 2000; Möller *et al.*, 2007; Martin *et al.*, 2008). Two Cretaceous analyses do not give reliable dates but the other four yield a pooled age of  $115.0 \pm 3.6$  (MSWD = 1.8). Eu and Ce concentrations are slightly greater than Stage 3, but have distinctly lower Th/U (< 0.1), as well as mol Y + REE (Fig. 9c,d).

### RELATIONSHIP OF MINERAL ASSEMBLAGES TO ZIRCON OVERGROWTHS

Zircon is an excellent geochronometer in high-grade terranes (e.g. Vavra *et al.*, 1996; Rubatto *et al.*, 2001; Rubatto, 2002; Möller *et al.*, 2003, 2007). The distribution of the overgrowths as rims to older grains points to formation during metamorphism (Corfu *et al.*, 2003; Hoskin & Schaltegger, 2003) and it would be convenient to directly assign Stage 3 ( $340.2 \pm 2.2$  Ma) and Stage 4 ( $115.0 \pm 3.6$  Ma) to M1 (moderate-*P*) and M2 (high-*P*), respectively. However, as zircon may not be affected during amphibolite facies metamorphism (Rubatto *et al.*, 2001), the metamorphic assemblages need to be tied directly to stages of

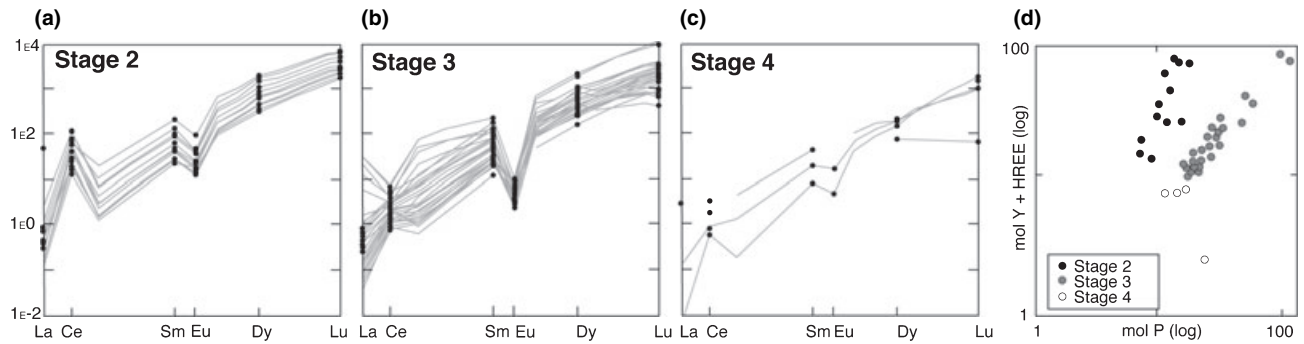


**Fig. 9.** (a–c) Chondrite-normalized REE profiles for zircon Stages 2–4. Profiles are constructed for measured (dots) and interpolated (lines) concentrations. One REE profile in (c) is partially obscured. Values below detection limit are omitted. (d). Subdivision of analyses by mol Y + heavy REE v. mol P.

zircon growth. Investigating trace element compositions of the zircon growth zones can do this.

Because the Stage 3 overgrowths truncate oscillatory zoning in Stage 1 and 2 zircon, and have unusual trace element concentrations, they most likely formed by open system processes and should have compositions that record interaction with metamorphic fluid (Martin *et al.*, 2008). Thus, if the Stage 3 zircon grew during M1, this population would be expected to have depleted heavy REE due to partitioning by the diffusion-zoned garnet (e.g. Schaltegger *et al.*, 1999; Rubatto, 2002; Hoskin & Schaltegger, 2003; Whitehouse & Platt, 2003; Kelly & Harley, 2005; Harley *et al.*, 2007; Rubatto & Herman, 2007) interpreted to have grown in the pelitic schist during this event. This is not the case; although some Stage 3 analyses show depletion in heavy REE, most do not (Fig. 9b). However, this model does not take into account the effects of metasomatism during M1, as indicated by formation of Al-enriched Lake Hankinson Complex directly at Marguerite Amphibolite margins. As the dated schist sample is a small (< 2 m) xenolith enclosed within M1-bearing layered amphibolite, the unusual depletion of Ce and Eu,  $\text{Th}/\text{U} > 1$ , and high heavy REE concentrations could reflect Stage 3 zircon having grown in equilibrium with fluid emanating from the surrounding amphibolite. A depletion of Ce in zircon is unusual but has been identified in amphibolite facies grains grown during metamorphism of a mafic intrusion (Schersten *et al.*, 2000). Zircon Ce concentration is mainly dependent on oxidation state (Ballard *et al.*, 2002) and the absence of Ce-repository minerals in either the pelitic schist or Marguerite Amphibolite suggests that the large Ce-depletion should be attributed to zircon formation in reducing conditions. Crystallization of M1 anorthite in the layered amphibolite under a reducing condition would also explain the low Eu concentration (Hoskin *et al.*, 2000; Ballard *et al.*, 2002; Hoskin & Schaltegger, 2003). High  $\text{Th}/\text{U}$ , which was achieved by increasing Th in the zircon lattice (Table S1), could have been achieved by mobilization of Th from primary amphibolite minerals. Therefore, the unusual Stage 3 zircon trace element characteristics

are consistent with growth in equilibrium with a reduced metasomatic fluid originating from the adjacent amphibolite during M1 and overwhelming the local signature of co-crystallizing garnet. Assigning an age of  $\sim 340$  Ma to M1 agrees with data from central and southern Fiordland, where kyanite-bearing pelitic schists have yielded Carboniferous monazite ages (Ireland & Gibson, 1998; Daczko *et al.*, 2009).

If Stage 4 grew in an open system during M2, then the zircon REE should reflect formation in equilibrium with the local high- $P$  assemblage. Although the Stage 4 overgrowths have lowered mol Y + heavy REE concentrations relative to the older zircon populations (Fig. 9d), they do not show the extreme depletion often recognized for zircon that has co-crystallized with garnet (Schaltegger *et al.*, 1999; Rubatto, 2002; Hoskin & Schaltegger, 2003; Whitehouse & Platt, 2003; Kelly & Harley, 2005; Harley *et al.*, 2007; Rubatto & Herman, 2007). However, as Stage 4 zircon overgrowth tend to follow pre-existing morphologies (Fig. 6) and have inherited compositions, these zones most likely formed by dissolution-precipitation in a closed system and hence should not have directly equilibrated with the metamorphic assemblages (Martin *et al.*, 2008). Independent evidence, however, indicates that M2 occurred at about the same time as the Stage 4 zircon growth. First, an upper age limit to M2 is given by the formation of Stage 4 zircon growth (between 118.8 and 111.2 Ma, with consideration of  $2\sigma$  errors) because it would be highly unlikely to recrystallize zircon and not affect the metamorphic assemblage in the same rock. The lower age bracket is given by the emplacement of a  $118.5 \pm 1.2$  Ma unmetamorphosed hornblende gabbro sill that intrudes M2-bearing rocks (Scott, *et al.*, in press). Therefore, M2 occurred at or after the age +  $2\sigma$  error of Stage 4 zircon (118.8 Ma) but before the age +  $2\sigma$  error of the hornblende gabbro sill (117.3 Ma). This result corresponds with the situation elsewhere in Fiordland, where static high- $P$  conditions are recognized to have occurred between 123 and 113 Ma (Mattinson *et al.*, 1986; Bradshaw, 1989; Hollis *et al.*, 2004; Daczko *et al.*, 2009).

In summary, cathodoluminescence imaging and LA-ICP-MS data obtained from zoned zircon grains provide evidence for the absolute timing of polyphase metamorphism. Zoned zircon from the Marguerite Amphibolite pelitic schist xenolith clearly demonstrates two metamorphic events – one in the Early Carboniferous and another in the Early Cretaceous. Simultaneous acquisition of zircon isotopes and trace elements by LA-ICP-MS depth-profiling, and correlation of the unusual trace element concentrations with proximal amphibolite M1 mineral assemblages, indicates the Stage 3 zircon grew in equilibrium with a metasomatic fluid during imposition of a pervasive lineated fabric at  $340.2 \pm 2.2$  Ma. On the other hand, although correlation of M2 and Stage 4 zircon is made on independent constraints, it is not verified by the zircon trace elements because the M2 event lacked penetrative deformation to drive recrystallization, fluid-enhanced element redistribution and open system zircon growth. This conclusion supports the findings of Martin *et al.* (2008), who showed that zircon growth-metamorphic assemblage correlation requires equilibration in an open system. Even in an open system, however, interpretation may be difficult if the host rock is proximal to a source of metasomatic fluid (as in the case of M1 in the Marguerite Amphibolite).

#### IMPLICATIONS FOR THE EVOLUTION OF A CONTINENTAL ARC

Examples of the preservation of older textures and mineral assemblages through later metamorphism are the persistence of quartz diorite or gabbro through blueschist or eclogite facies conditions because of the absence of deformation and infiltration of fluid (Koons *et al.*, 1987; Rubie, 1998; Engvik *et al.*, 2001; John & Schenk, 2003). Although not attaining eclogite facies conditions, the Marguerite Amphibolite is an example of how early assemblages have persisted through the growth of a continental arc at moderate-*P*. Small patches of corona-bearing gabbro occur in low strain domains that avoided re-equilibration despite M1 being associated with element redistribution, as illustrated by the unusual Stage 3 zircon compositions and the hybrid Al-enriched Lake Hankinson Complex at the margins of the amphibolite xenoliths. The gabbro represents the protolith to some of the amphibolites because it clearly grades into amphibolite (Fig. 2d). Therefore, even though M1 reactions generally ran to completion and thorough reconstitution is represented by lineated layered amphibolite, small low strain domains retained igneous textures.

The Marguerite Amphibolite also shows that pre-existing metamorphic assemblages can persist metastably through a high-*P* event in a continental arc setting. Although Early Cretaceous high-*P* assemblages (M2) do occur, lineated moderate-*P* (M1) Carboniferous assemblages dominate. The retention of M1 assemblages is attributed to a lack of deformation

and the limited influence of metamorphic fluids in redistributing elements during M2. Evidence for this is the static nature of M2 assemblages, the pseudomorphing of igneous gabbro coronas (Fig. 4b) by M2 minerals with compositions such as  $X_{Mg}$  and  $SiO_2$  similar to their igneous precursors, and by the growth of Stage 4 zircon in a closed system. Factors controlling the lack of deformation and fluid infiltration may be the short duration of peak *P-T* and large distance (up to 9 km for parts of the Marguerite Amphibolite) from Early Cretaceous heat sources (Brown, 1996). For example, the thin and discontinuous high-*P* garnet rims in pelitic schist indicate cooling before diffusion zoning took place (Tracy, 1982), and hence that the M2 event was maintained for only a short time. This is in accordance with the known evolution of the Fiordland lower crust, which has high-*P* metamorphism (123–113 Ma) closely followed by isobaric cooling (113–111 Ma) and then extensional exhumation (111–90 Ma) (Gibson *et al.*, 1988; Daczko *et al.*, 2002c; Flowers *et al.*, 2005; Scott & Cooper, 2006). The distance from Early Cretaceous mafic batholiths (WFO and ARC) that would have acted as additional heat sources during M2, provides an explanation for why rocks within and at the margins of these batholiths record high-*P* metamorphism (Bradshaw, 1989; Clarke *et al.*, 2000; Daczko *et al.*, 2002a; Hollis *et al.*, 2004) but rocks some distance away tend to contain a partial record at best (Brown, 1996; Daczko *et al.*, 2009; this study). The apparent absence of a peak metamorphic assemblage does not rule out a polyphase polybaric metamorphic history, only that there was no (or only very little) recrystallization. In cases where there is evidence for a short duration of peak *P-T*, a large distance from a heat source, or a lack of penetrative deformation, the possibility of metastability should be considered.

#### IMPLICATIONS FOR THE FIORDLAND GONDWANA MARGIN

Mineralogy and *P-T* estimates from the Marguerite Amphibolite and associated rocks show that the Gondwana margin in northern Fiordland was affected by two phases of kyanite-grade metamorphism. The first event (M1) occurred at moderate *P-T* ( $6.6 \pm 0.8$  kbar,  $618 \pm 25$  °C) at  $340.2 \pm 2.2$  Ma and has not previously been established in northern Fiordland. One line of evidence cited for a ~6 kbar Early Cretaceous burial event of the Fiordland crust comes from the different core and rim composition of garnet grains in pelitic schist xenoliths within the WFO (Bradshaw, 1989, 1991; Brown, 1996). However, these grains are strikingly similar to those described from within the pelitic schist enclosed in Marguerite amphibolite. As the garnet cores identified in this schist are inferred to represent Carboniferous growth, age inferences for other examples of Fiordland zoned garnet, in the absence of geochronological data, should be treated with extreme care.

Northern Fiordland was subject to collision of an outboard magmatic arc in the Early Cretaceous, accompanied by emplacement of vast volumes of magma and high-*P* metamorphism, and closely followed by rapid regional decompression. This dramatic evolution is only recorded in the Marguerite Amphibolite by sparse static metamorphic textures. Carboniferous assemblages were retained because the lack of penetrative deformation resulted in little element redistribution and recrystallization during high-*P* conditions, and was aided by a short residence time of the crust at peak *P–T* and distance from heat sources. Brown (1996) and Daczko *et al.* (2009) reached similar conclusions for sections of the arc in southwest Fiordland. Therefore, although many parts of the Fiordland continental arc do not show evidence for Early Cretaceous high-*P* equilibration, it is possible that many of these areas (which mostly contain less sensitive bulk compositions than the rocks of this study) attained high-*P* conditions but maintained earlier metamorphic or igneous assemblages throughout this dramatic orogenic cycle.

#### ACKNOWLEDGEMENTS

A GNS Science Origin of the Continental Crust PhD Scholarship, a Hastie Award, an Otago Travel Grant and the Benson Fund supported work by JMS. Otago Research Grants to JMP covered zircon analyses, which were conducted under the guidance of C. Allen at the Australian National University. R. Fairhurst provided excellent help with microprobe analyses and M. Holdaway generously made available his GB-GASP program. Critical comments by A. Allibone, N. Daczko, P. Hoskin, K. Klepeis, D. Robinson, H. Stowell, I. Turnbull, A. Tulloch, P. Upton, R. Wysoczanski and two anonymous reviewers are very much appreciated.

#### REFERENCES

- Allibone, A. H., Turnbull, I. M., Tulloch, A. J. & Cooper, A. F., 2007. Plutonic rocks of the Median Batholith in southwest Fiordland, New Zealand: field relations, geochemistry, and correlation. *New Zealand Journal of Geology and Geophysics*, **50**, 283–314.
- Arnold, J., Powell, R. & Sandiford, M., 2000. Amphibolites with staurolite and other aluminous minerals: calculated mineral equilibria in NCFMASH. *Journal of Metamorphic Geology*, **18**, 23–40.
- Ballard, J. R., Palin, J. M. & Campbell, I. H., 2002. Relative oxidation states of magmas inferred from Ce(IV)/Ce(III) in zircon; application to porphyry copper deposits of northern Chile. *Contributions to Mineralogy and Petrology*, **144**, 347–364.
- Blattner, P., 1991. The North Fiordland transcurrent convergence. *New Zealand Journal of Geology and Geophysics*, **34**, 533–542.
- Blattner, P. & Graham, I. J., 2000. New Zealand's Darran Complex and Mackay Intrusives – Rb-Sr whole rock isochrons in the Median Tectonic Zone. *American Journal of Science*, **300**, 603–629.
- Bradshaw, J. Y., 1989. Origin and metamorphic history of a polybaric granulite terrain, Fiordland, southwest New Zealand. *Contributions to Mineralogy and Petrology*, **103**, 346–360.
- Bradshaw, J. Y., 1990. Geology of crystalline rocks of Northern Fiordland: details of the granulite facies Western Fiordland Orthogneiss and associated rock units. *New Zealand Journal of Geology and Geophysics*, **33**, 465–484.
- Bradshaw, J. Y., 1991. Zoned garnets in metapelites in western Fiordland, southwest New Zealand: polychronic crystallisation and insight into the nature and extent of Early Cretaceous regional metamorphism. *New Zealand Journal of Geology and Geophysics*, **34**, 261–270.
- Bradshaw, J. D., 1993. A review of the Median Tectonic Zone: terrane boundaries and terrane amalgamation near the Median Tectonic Line. *New Zealand Journal of Geology and Geophysics*, **36**, 117–125.
- Brown, E. H., 1996. High-pressure metamorphism caused by magma loading in Fiordland, New Zealand. *Journal of Metamorphic Geology*, **14**, 441–452.
- Chatterjee, N. D., Johannes, W. & Leistner, H., 1984. The system CaO-Al<sub>2</sub>O<sub>3</sub>-SiO<sub>2</sub>-H<sub>2</sub>O: new phase equilibria data, some calculated phase relations, and their petrological applications. *Contributions to Mineralogy and Petrology*, **88**, 1–13.
- Clarke, G. L., Daczko, N. R., Klepeis, K. A. & Rushmes, T., 2005. Roles for fluid and/or melt advection in forming high-*P* matic migmatites, Fiordland, New Zealand. *New Zealand Journal of Metamorphic Geology*, **23**, 557–567.
- Clarke, G. L., Klepeis, K. A. & Daczko, N. R., 2000. Cretaceous high-*P* granulites at Milford Sound, New Zealand: metamorphic history and emplacement in a convergent margin setting. *Journal of Metamorphic Geology*, **18**, 359–374.
- Claypool, A. L., Klepeis, K. A., Dockrill, B., Clarke, G. L., Zwingmann, H. & Tulloch, A., 2002. Structure and kinematics of oblique convergence in northern Fiordland, New Zealand. *Tectonophysics*, **359**, 329–358.
- Compston, W., Williams, I. S. & Meyer, C., 1984. U-Pb geochronology of zircons from lunar breccia 73217 using a sensitive high mass-resolution ion microprobe. *Journal of Geophysical Research*, **89**(Suppl.), B524–B525.
- Corfu, F., Hanchar, J. M., Hoskin, P. W. O. & Kinney, P. D., 2003. Atlas of zircon textures. In: *Zircon* (eds Hanchar, J. M. & Hoskin, P. W. O.) *Reviews in Mineralogy and Geochemistry*, **53**, Mineralogical society of America, Washington, DC, 468–501.
- Daczko, N. R. & Halpin, J. A., 2009. Evidence for melt migration enhancing recrystallization of metastable assemblages in mafic lower crust, Fiordland, New Zealand. *Journal of Metamorphic Geology*, **27**, 167–185.
- Daczko, N. R., Klepeis, K. A. & Clarke, G. L., 2001a. Evidence of Early Cretaceous collisional-style orogenesis in northern Fiordland, New Zealand and its effects on the evolution of the lower crust. *Journal of Structural Geology*, **23**, 673–713.
- Daczko, N. R., Klepeis, K. A. & Clarke, G. L., 2001b. Transformation of two-pyroxene hornblende granulite to garnet granulite involving simultaneous melting and fracturing of the lower crust, Fiordland, New Zealand. *Journal of Metamorphic Geology*, **19**, 549–562.
- Daczko, N. R., Stevenson, J. A., Clarke, G. L. & Klepeis, K. A., 2002a. Successive hydration and dehydration of high-*P* mafic granulites involving clinopyroxene-kyanite symplectites, Mt Daniel, Fiordland, New Zealand. *Journal of Metamorphic Geology*, **20**, 669–682.
- Daczko, N. R., Klepeis, K. A. & Clarke, G. L., 2002b. Thermochronological evolution of the crust during convergence and deep crustal pluton emplacement in the Western Province of Fiordland, New Zealand. *Tectonics*, **21**, 1–17.
- Daczko, N. R., Clarke, G. L. & Klepeis, K. A., 2002c. Kyanite-paragonite-bearing assemblages, northern Fiordland, New Zealand: rapid cooling of the lower crustal root to a Cretaceous magmatic arc. *Journal of Metamorphic Geology*, **20**, 887–902.

- Daczko, N. R., Milan, L. A. & Halpin, J. A., 2009. Metastable persistence of pelitic metamorphic assemblages at the root of a Cretaceous magmatic arc – Fiordland New Zealand. *Journal of Metamorphic Geology*, **27**, 233–247.
- Davids, C., 1999. *A Thermochemical Study of Southern Fiordland, New Zealand*. PhD Thesis, Australian National University, Canberra.
- Engvik, A. K., Austrheim, H. & Erambert, M., 2001. Interaction between fluid flow, fracturing and mineral growth during eclogitization, an example from the Sunnfjord area, Western Gneiss Region, Norway. *Lithos*, **57**, 111–141.
- Ewing, T. A., Weaver, S. D., Bradshaw, J. D., Turnbull, I. M. & Ireland, T. R., 2007. Loch Burn Formation, Fiordland, New Zealand: SHRIMP U-Pb ages, geochemistry and provenance. *New Zealand Journal of Geology and Geophysics*, **50**, 167–180.
- Flowers, R. M., Bowring, S. A., Tulloch, A. J. & Klepeis, K. A., 2005. Tempo of burial and exhumation within the deep roots of a magmatic arc, Fiordland, New Zealand. *Geology*, **33**, 17–20.
- Gibson, G. M., 1982. Polyphase deformation and its relationship to metamorphic crystallisation in rocks at Wilmot Pass, Fiordland, New Zealand. *New Zealand Journal of Geology and Geophysics*, **25**, 45–65.
- Gibson, G. M., 1990. Uplift and exhumation of middle to lower crustal rocks in an extensional setting, Fiordland, New Zealand. In: *Exposed cross-sections of the continental crust*, (eds Salisbane, M. H. & Fountation, O. M.), *NATO ASI Series*, **C317**, 145–157.
- Gibson, G. M. & Ireland, T. R., 1995. Granulite formation during continental extension in Fiordland, New Zealand. *Nature*, **375**, 479–482.
- Gibson, G. M. & Ireland, T. R., 1996. Extension of the Delamerian (Ross) Orogen into western New Zealand; evidence from zircon ages and implications for crustal growth along the Pacific margin of Gondwana. *Geological Society of America bulletin*, **24**, 1087–1090.
- Gibson, G. M., McDougall, I. & Ireland, T. R., 1988. Age constraints on metamorphism and the development of a metamorphic core complex in Fiordland, southern New Zealand. *Geology*, **16**, 405–408.
- de Haas, G.-J. L., Nijland, T. G., Valbracht, P., Maijer, C., Vershure, R. & Anderson, T., 2002. Magmatic versus metamorphic origin for olivine-plagioclase coronas. *Contributions to Mineralogy and Petrology*, **143**, 537–550.
- Harley, S. L., Kelly, N. M. & Moller, A., 2007. Zircon behaviour and the thermal histories of mountain chains. *Elements*, **3**, 25–30.
- Holdaway, M. J., 2000. Application of new experimental and garnet Margules data to the garnet-biotite geothermometer. *American Mineralogist*, **85**, 881–892.
- Holdaway, M. J., 2001. Recalibration of the GASP geobarometer in light of recent garnet and plagioclase activity models and versions of the garnet-biotite geothermometer. *American Mineralogist*, **86**, 1117–1129.
- Holland, T. J. B. & Powell, R., 1998. An internally consistent thermodynamic data set for phases of petrological interest. *Journal of Metamorphic Geology*, **16**, 309–343.
- Hollis, J. A., Clarke, G. L., Klepeis, K. A., Daczko, N. R. & Ireland, T. R., 2003. Geochronology and geochemistry of high-pressure granulites of the Arthur River Complex, Fiordland, New Zealand: Cretaceous magmatism and metamorphism on the palaeo-Pacific Margin. *Journal of Metamorphic Geology*, **21**, 299–313.
- Hollis, J. A., Clarke, G. L., Klepeis, K. A., Daczko, N. R. & Ireland, T. R., 2004. The regional significance of Cretaceous magmatism and metamorphism in Fiordland, New Zealand, from U-Pb zircon geochronology. *Journal of Metamorphic Geology*, **22**, 607–627.
- Hoskin, P. W. O. & Black, L. P., 2000. Metamorphic zircon formation by solid-state recrystallization of protolith igneous zircon. *Journal of Metamorphic Geology*, **18**, 423–439.
- Hoskin, P. W. O. & Schaltegger, U., 2003. The composition of zircon and igneous and metamorphic petrogenesis. In: *Zircon* (eds Hanchar, J. M. & Hoskin, P. W. O.), *Reviews in Mineralogy and Geochemistry*, **53**, Mineralogical society of America, Washington, DC, 27–62.
- Hoskin, P. W. O., Kinny, P. D., Wyborn, D. & Chappell, B. W., 2000. Identifying accessory mineral saturation during differentiation in granitoid magmas: an integrated approach. *Journal of Petrology*, **41**, 1365–1396.
- House, M. A., Gurnis, M., Kamp, P. J. J. & Sutherland, R., 2002. Uplift in the Fiordland Region, New Zealand: Implications for Incipient Subduction. *Science*, **297**, 2038–2041.
- House, M. A., Gurnis, M., Sutherland, R. & Kamp, P. J., 2005. Patterns of Late Cenozoic exhumation deduced from apatite and zircon U-He ages from Fiordland, New Zealand. *Geochemistry, Geophysics, Geosystems*, **6**, 13.
- Ireland, T. R. & Gibson, G. M., 1998. SHRIMP monazite and zircon geochronology of high-grade metamorphism in New Zealand. *Journal of Metamorphic Geology*, **16**, 149–167.
- John, T. & Schenk, V., 2003. Partial eclogitisation of gabbroic rocks in a late Precambrian subduction zone (Zambia): prograde metamorphism triggered by fluid infiltration. *Contributions to Mineralogy and Petrology*, **146**, 174–191.
- Jongens, R., Bradshaw, J. D. & Fowler, A. P., 2003. The Balloon Melange, northwest Nelson: origin, structure and emplacement. *New Zealand Journal of Geology and Geophysics*, **46**, 437–448.
- Kelly, N. M. & Harley, S. L., 2005. An integrated microtextural and chemical approach to zircon geochronology: refining the Archaean history of the Napier Complex, east Antarctica. *Contributions to Mineralogy and Petrology*, **149**, 57–84.
- Kimbrough, D. L., Tulloch, A. J., Coombs, D. S., Landis, C. A., Johnston, M. R. & Mattinson, J. M., 1994. Uranium-lead ages from the Median Tectonic Zone, New Zealand. *New Zealand Journal of Geology and Geophysics*, **37**, 303–319.
- King, R. P., 1984. *Some Aspects of the Geology of the George Sound Track Area, North-Central Fiordland*. M.Sc. Thesis, University of Otago, Dunedin.
- Klepeis, K. A., King, D., de Paoli, M., Clarke, G. L. & Gehrels, G., 2007. Interaction of strong lower and weak middle crust during lithospheric extension in western New Zealand. *Tectonics*, **26**, TC4017.
- Koons, P. O., Rubie, D. C. & Frueh-Green, G., 1987. The effects of disequilibrium and deformation on the mineralogical evolution of quartz diorite during metamorphism in the eclogite facies. *Journal of Petrology*, **28**, 679–700.
- Landis, C. A. & Coombs, D. S., 1967. Metamorphic belts and orogenesis in southern New Zealand. *Tectonophysics*, **4**, 501–518.
- Leake, B. E., Woolley, A. R., Arps, C. E. S. *et al.*, 1997. Nomenclature of amphiboles: report of the subcommittee on amphiboles of the International Mineralogical Association commission on new minerals and mineral names. *The Canadian Mineralogist*, **33**, 219–246.
- Martin, L. A. J., Duchene, S., Deloule, E. & Vanderhaeghe, O., 2008. Mobility of trace elements and oxygen during metamorphism: consequences for geochemical tracing. *Earth and Planetary Science Letters*, **267**, 161–174.
- Mattinson, J. M., Kimbrough, D. L. & Bradshaw, J. Y., 1986. Western Fiordland orthogneiss: early Cretaceous arc magmatism and granulite facies metamorphism, New Zealand. *Contributions to Mineralogy and Petrology*, **92**, 383–392.
- Möller, A., O'Brien, P. J., Kennedy, A. & Kroener, A., 2003. Linking growth episodes of zircon and metamorphic textures to zircon chemistry: an example from the ultrahigh-temperature granulites of Rogaland (SW Norway). In: *Geochronology: Linking the Isotopic Record with Petrology and Textures* (eds Vance, D., Moller, W. & Villa, I. M.), *Geological Society, London, Special Publications*, **220**, 65–81.
- Möller, C., Andersson, J., Lundqvist, I. & Hellstrom, F., 2007. Linking deformation, migmatite formation and zircon U-Pb geochronology in polymetamorphic orthogneisses, Svencorwegian Province, Sweden. *Journal of Metamorphic Geology*, **25**, 727–750.

- Mortimer, N., 2004. New Zealand's Geological Foundations. *Gondwana Research*, **7**, 261–272.
- Mortimer, N., Gans, P., Calvert, A. & Walker, N., 1999a. Geology and thermochronometry of the east edge of the Median Batholith (Median Tectonic Zone): a new perspective on the Permian to Cretaceous crustal growth of New Zealand. *The Island Arc*, **8**, 404–425.
- Mortimer, N., Tulloch, A. J., Spark, R. N. *et al.*, 1999b. Overview of the geology of the Median Tectonic Zone and adjacent rocks. *Journal of African Earth Sciences*, **29**, 257–268.
- Muir, R. J., Ireland, T. R., Weaver, S. D. *et al.*, 1998. Geochronology and Geochemistry of a Mesozoic magmatic arc system, Fiordland, New Zealand. *Journal of the Geological Society of London*, **155**, 1037–1053.
- Oliver, G. J. H., 1977. Feldspathic hornblende and garnet granulites and associated anorthositic pegmatites from Doubtful Sound, Fiordland New Zealand. *Contributions to Mineralogy and Petrology*, **65**, 111–121.
- Powell, R. & Holland, T. J. B., 1994. Optimal geothermometry and geobarometry. *American Mineralogist*, **79**, 120–133.
- Rubatto, D., 2002. Zircon trace element geochemistry: partitioning with garnet and the link between U-Pb ages and metamorphism. *Chemical Geology*, **184**, 123–138.
- Rubatto, D. & Herman, J., 2007. Experimental zircon/melt and zircon/garnet trace element partitioning and implications for the geochronology of crustal rocks. *Chemical Geology*, **241**, 38–61.
- Rubatto, D., Williams, I. S. & Buick, I. S., 2001. Zircon and monazite response to prograde metamorphism in the Reynolds Range, central Australia. *Contributions to Mineralogy and Petrology*, **140**, 458–468.
- Rubie, D. C., 1998. Disequilibrium during metamorphism: the role of nucleation kinetics. In: *What Drives Metamorphism and Metamorphic Reactions?* (eds Treloar, P. J. & O'Brien, P.). *Geological Society, London, Special Publications*, **138**, 199–214.
- Schaltegger, U., Fanning, C. M., Gunther, D., Maurin, J. C., Schulmann, K. & Gebauer, D., 1999. Growth, annealing and recrystallization of zircon and preservation of monazite in high-grade metamorphism: conventional and in-situ U-Pb isotope, cathodoluminescence and microchemical evidence. *Contributions to Mineralogy and Petrology*, **134**, 186–201.
- Schersten, A., Areback, H., Cornell, D., Hoskin, P., Aberg, A. & Armstrong, R., 2000. Dating mafic-ultramafic intrusions by ion-microprobing contact-melt zircon: examples from SW Sweden. *Contributions to Mineralogy and Petrology*, **139**, 115–125.
- Scott, J. M., 2008. *Tectonic Evolution of the Eastern Fiordland Gondwana Margin*. PhD thesis, University of Otago, Dunedin.
- Scott, J. M. & Cooper, A. F., 2006. Early Cretaceous extensional exhumation of the lower crust of a magmatic arc: Evidence from the Mount Irene Shear Zone, Fiordland, New Zealand. *Tectonics*, **25**, TC3018.
- Scott, J. M. & Palin, J. M., 2008. LA-ICP-MS U-Pb zircon dates from Mesozoic plutonic rocks in eastern Fiordland, New Zealand. *New Zealand Journal of Geology and Geophysics*, **51**, 105–113.
- Scott, J. M., Palin, J. M. & Cooper, A. F., in press. A younger age constraint on high-grade metamorphism near George Sound in Fiordland, New Zealand. *New Zealand Journal of Geology and Geophysics*, **52**.
- Scott, J. M., Turnbull, I. M., Ewing, T. A., Allibone, A. H., Palin, J. M. & Cooper, A. F., 2008. Petrogenesis and geochronology of the volcanoclastic and volcanogenic Mesozoic Loch Burn Formation in eastern Fiordland, New Zealand. *New Zealand Journal of Geology and Geophysics*, **51**, 89–103.
- Siivola, J. & Schmidt, R., 2007. *List of Mineral Abbreviations, IUGS Subcommission on the Systematics of Metamorphic Rocks*. Available at: <http://www.bgs.ac.uk/scmr/home.html> (last accessed on 1 February 2007).
- Spear, F. S., Kohn, M. J. & Cheney, J. T., 1999. P-T paths from anatectic pelites. *Contributions to Mineralogy and Petrology*, **134**, 17–32.
- Tracy, R. J., 1982. Compositional zoning and inclusions in metamorphic minerals. In: *Characterization of Metamorphism through Mineral Equilibria* (ed. Ferry, J. M.). *Mineralogical Society of America, Reviews in Mineralogy*, **10**, 397.
- Tsujimori, T. & Liou, J. G., 2004. Metamorphic evolution of kyanite-staurolite-bearing epidote-amphibolite from the Early Palaeozoic Oeyama belt, SW Japan. *Journal of Metamorphic Geology*, **22**, 301–313.
- Vavra, G., Gebauer, D., Schmid, R. & Compston, W., 1996. Multiple zircon growth and recrystallisation during polyphase Late Carboniferous to Triassic metamorphism in granulites of the Ivrea Zone (Southern Alps): an ion microprobe (SHRIMP) study. *Contributions to Mineralogy and Petrology*, **122**, 337–358.
- Wandres, A. M. & Bradshaw, J. D., 2005. New Zealand tectonostratigraphy and implications from conglomeratic rocks for the configuration of the SW Pacific margin of Gondwana. In: *Terrane Processes at the Margins of Gondwana*, (eds Vaughan, A. P. M., Leat, P. T. & Pankhurst, R. J.). *Geological Society, London, Special Publications*, **246**, 179–216.
- Whitehouse, M. J. & Platt, J. P., 2003. Dating high-grade metamorphism—constraints from rare-earth elements in zircon and garnet. *Contributions to Mineralogy and Petrology*, **145**, 61–74.
- Williams, J. G., 1978. Eglington Volcanics – stratigraphy, petrography and metamorphism. *New Zealand Journal of Geology and Geophysics*, **21**, 733–742.
- Williams, J. G. & Harper, C. T., 1978. Age and status of the Mackay Intrusives in the Eglington-Upper Hollyford area. *New Zealand Journal of Geology and Geophysics*, **21**, 733–742.

## SUPPORTING INFORMATION

Additional Supporting Information may be found in the online version of this article:

**Table S1.** U-Th-Pb zircon data from sample OU 41573.

Please note: Wiley-Blackwell are not responsible for the content or functionality of any supporting materials supplied by the authors. Any queries (other than missing material) should be directed to the corresponding author for the article.

Received 14 January 2009; revision accepted 20 March 2009.